

Aggregation in solution of neutral half-sandwich Ru(II) precatalysts for transfer hydrogenation†

Daniele Zuccaccia,^a Eric Clot^{*b} and Alceo Macchioni^{*a}

^a Dipartimento di Chimica, Università di Perugia, via Elce di Sotto, 8, 06123 Perugia, Italy.

E-mail: alceo@unipg.it; Fax: (+)39 075 585 5598; Tel: (+)39 075 585 5579

^b LSDSMS (CNRS UMR 5636), Université Montpellier 2, Case Courrier 14, Place E.

Bataillon, 34095 Montpellier cedex 5, France E-mail: clot@univ-montp2.fr;

Fax: (+)33 467 14 48 39; Tel: (+)33 467 14 39 14

Received (in Montpellier, France) 7th October 2004, Accepted 16th November 2004

First published as an Advance Article on the web 21st January 2005

Diffusion NMR measurements and ONIOM (B3PW91:UFF) calculations show that amino amidate and acidate half-sandwich Ru(II) precatalysts for transfer hydrogenation have a remarkable tendency to form dimers and even larger aggregates in several solvents, including isopropanol, that is, the solvent used in the catalysis reaction.

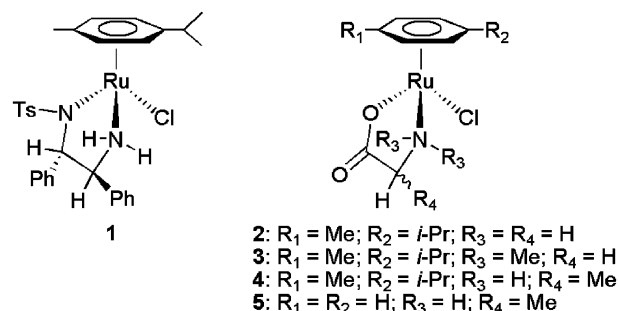
The neutral ruthenium complexes presented in Scheme 1 have been successfully applied as catalysts in transfer hydrogenation of ketones.^{1,2} In-depth studies indicated that a key role in the catalytic processes is played by second-sphere interactions between the to-be-activated substrates and ligand functionalities.¹ In particular, the amino amidate or α -amino acidate ligands present in the precatalysts are ideally suited to establish hydrogen bonds (HB) with the substrates, either as HB-donors (N–H) or HB-acceptors (S=O or C=O). Moreover, the Ru–Cl linkage is also prone to be engaged in HB patterns.³ The N–H...Y (Y = O, Cl) HB can also occur between two ruthenium complexes, as observed in the solid state.⁴ Interestingly, even when N–H acidic protons are not present, half-sandwich Ru(II) complexes tend to form inversion pairs in the solid state.⁵ In this case, the HB pattern involves the less acidic C–H protons on the substituted benzene ring and the electronegative Y atoms coordinated to Ru.⁵

In solvents with medium to high relative permittivity (methanol, acetone, isopropanol, DMSO), the H-bonding interactions are expected to occur between a single Ru complex and solvent molecules. However, our previous NMR studies indicated that half-sandwich ruthenium(II) salts, [Ru(η^6 -arene)(N,N)Cl]⁺X[–] (N,N = α -diimine), not only are mainly present as ion pairs in a broad range of solvents but they also significantly form ion quadruples through the association of two ion pairs.⁶ In addition, while when X[–] = BPh₄[–] the ion quadruples have the expected (– + – +) structure with one anion bridging two cationic moieties, when X[–] = BF₄[–] ion quadruples of the (– + + –) type are present in solution, most likely held together by efficient H-bonding interactions between the cationic moieties of two ion pairs.⁶ We thus decided to extend our studies to neutral systems and explore the possibility that the latter can undergo aggregation in solution.

Here we show, for the first time, that the precatalysts for transfer hydrogenation reported in Scheme 1 (Ts = *p*-CH₃C₆H₄SO₂) have a marked tendency to form dimers and

larger aggregates in several solvents, including isopropanol, the solvent used in the catalysis reaction.

The aggregation tendency of compounds **1–5** (Scheme 1) and *trans*-[Ru(COMe)(CO)[(pz)₂BH₂](PMe₃)₂] (**6**)⁷ (pz = pyrazol-1-yl) was studied by the pulsed field gradient spin-echo (PGSE) NMR technique (see Electronic Supplementary Information, ESI).⁸ This technique allows the translational self-diffusion coefficient (*D*_t) to be determined. *D*_t is related to the hydrodynamic radius (*r*_H) of the diffusing particle, according to a modified Stokes–Einstein equation: *D*_t = *kT*/cπη*r*_H (where *k* is the Boltzmann constant, *T* is the temperature, *c* is a numerical factor that can be expressed as a function of *r*_H and the van der Waals radius of the solvent⁹ and η is the solution viscosity). From the experimentally determined *D*_t values, *r*_H, *c* and the hydrodynamic volumes (*V*_H) of the species present in solution were estimated. The ratio between *V*_H and the van der Waals volume (*V*_{vdw}) afforded the aggregation number *N*. Corresponding data are reported in Table 1. Compounds **1–5** show an aggregation number *N* significantly higher than one (entries 1–22), while *N* is close to one for the reference compound **6** in all investigated solvents (entries 23–27). The observation of *N* values greater than one in solvents of a different nature and their dependence on the concentration of complexes **1–5** clearly indicate that solvation is not the main factor responsible for the observed large hydrodynamic volumes. On the contrary, such observations suggest that half-sandwich complexes **1–5** have a strong tendency to form molecular adducts, even at the lowest investigated concentration of 0.05 mM (entry 1), in isopropanol-*d*₈ (relative permittivity $\epsilon_r^{298\text{ K}}$ = 19.92). Noyori's precatalyst (*S,S*)-**1** (*V*_{vdw} = 459 Å³, *r*_{vdw} = 4.8 Å)¹⁰ has an aggregation number *N* equal to 1.8, indicative of the presence of mainly dimers. Increasing concentration (entries 2–6, Fig. 1) leads to further aggregation, up to tetramers for the saturated solution (entry 6, *N* = 4.0).



Scheme 1

† Electronic Supplementary Information (ESI) available: details of PGSE NMR measurements for **1–6**. See <http://www.rsc.org/suppdata/nj/b4/b415560b/>.

Table 1 Diffusion coefficients (D_t), hydrodynamic radii (r_H), c factors, hydrodynamic volumes (V_H) and aggregation numbers (N) as a function of concentration (C) in isopropanol- d_8 (unless noted otherwise)

| Entry | Compound | $10^{10} D_t / \text{m}^2 \text{s}^{-1}$ | $r_H / \text{\AA}$ | c | $V_H / \text{\AA}^3$ | N | C / mM |
|-------|----------------|--|--------------------|-----|----------------------|-----|-------------------|
| 1 | 1 | 1.6 | 5.8 | 5.2 | 833 | 1.8 | 0.05 |
| 2 | 1 | 1.6 | 5.8 | 5.2 | 842 | 1.8 | 0.2 |
| 3 | 1 | 1.6 | 6.2 | 5.2 | 988 | 2.1 | 1.0 |
| 4 | 1 | 1.5 | 6.3 | 5.3 | 1051 | 2.3 | 4.0 |
| 5 | 1 | 1.4 | 6.7 | 5.4 | 1264 | 2.8 | 12.0 |
| 6 | 1 | 1.1 | 7.6 | 5.5 | 1823 | 4.0 | 42.0 ^a |
| 7 | 1 ^b | 6.1 | 6.4 | 5.5 | 1087 | 2.4 | 2.0 |
| 8 | 1 ^b | 4.6 | 8.1 | 5.7 | 2242 | 4.9 | 12.0 |
| 9 | 1 ^c | 11.4 | 5.8 | 5.3 | 815 | 1.8 | 2.0 |
| 10 | 1 ^d | 6.3 | 5.8 | 5.5 | 834 | 1.8 | 2.0 |
| 11 | 1 ^e | 1.6 | 6.6 | 5.5 | 1204 | 2.6 | 2.0 |
| 12 | 2 | 2.0 | 5.1 | 4.9 | 572 | 2.6 | 0.5 |
| 13 | 2 | 1.9 | 5.3 | 5.0 | 623 | 2.8 | 1.5 |
| 14 | 2 | 1.9 | 5.3 | 5.0 | 630 | 2.8 | 4.0 ^a |
| 15 | 3 | 2.4 | 4.7 | 4.7 | 443 | 1.7 | 0.2 |
| 16 | 3 | 2.1 | 4.9 | 4.8 | 492 | 1.9 | 4.0 |
| 17 | 3 | 2.1 | 4.9 | 4.8 | 501 | 2.0 | 7.0 ^a |
| 18 | 3 ^e | 2.5 | 4.6 | 5.0 | 415 | 1.7 | 2.6 |
| 19 | 4 | 1.9 | 5.3 | 5.0 | 613 | 2.6 | 9.0 |
| 20 | 4 | 1.6 | 5.9 | 5.2 | 847 | 3.6 | 50.0 |
| 21 | 5 | 2.1 | 4.9 | 4.8 | 480 | 2.7 | 0.5 ^a |
| 22 | 5 ^e | 2.2 | 4.9 | 5.1 | 498 | 2.7 | 60.0 |
| 23 | 6 | 2.5 | 4.6 | 4.7 | 410 | 1.1 | 2.0 |
| 24 | 6 ^b | 9.2 | 4.7 | 5.1 | 470 | 1.2 | 2.0 |
| 25 | 6 ^b | 8.5 | 4.7 | 5.1 | 448 | 1.2 | 16.0 |
| 26 | 6 ^d | 8.6 | 4.7 | 5.0 | 451 | 1.2 | 2.0 |
| 27 | 6 ^f | 8.2 | 4.4 | 4.9 | 368 | 1.0 | 2.0 |

^a Saturated solution. ^b In CDCl_3 . ^c In acetone- d_6 . ^d In methanol- d_4 . ^e In DMSO- d_6 . ^f In benzene- d_6 .

The aggregation tendency of compound **1** is not limited to isopropanol- d_8 as aggregation was also observed in CDCl_3 ($\epsilon_r^{293 \text{ K}} = 4.81$, entries 7–8), acetone- d_6 ($\epsilon_r^{298 \text{ K}} = 20.56$, entry 9), methanol- d_4 ($\epsilon_r^{298 \text{ K}} = 32.66$, entry 10) and DMSO- d_6 ($\epsilon_r^{298 \text{ K}} = 46.45$, entry 11). In all solvents, at a concentration of 2 mM, the aggregation number N is close to two, indicating that the dimeric structure of compound **1** is always the most stable, independent of the solvent polarity and nature. In the solid state,¹⁰ short $\text{NH} \cdots \text{O}^1\text{SO}^2$ (2.16 Å) and $\text{CH} \cdots \text{O}^2\text{SO}^1$ (2.61 and 2.81 Å) intermolecular hydrogen bonds are present between two ruthenium units. Starting from the experimental data,¹⁰ ONIOM (B3PW91:UFF) calculations were carried out on the dimeric structure **1–1**. Fig. 2 shows the optimized geometry, in which the short $\text{NH} \cdots \text{O}1$ (2.14 Å) and $\text{CH} \cdots \text{O}2$

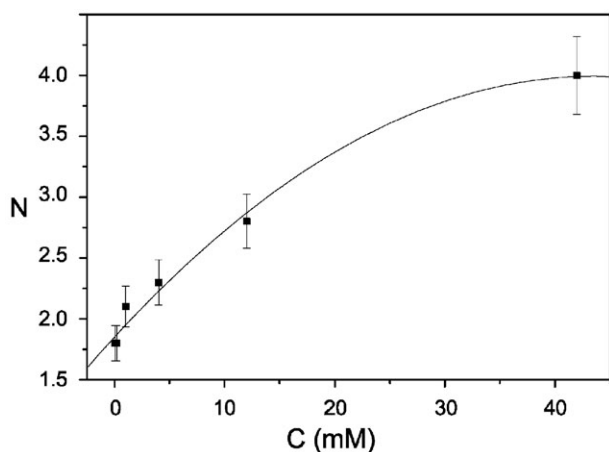


Fig. 1 Aggregation number (N) as a function of the concentration in isopropanol- d_8 at 296 K for compound **1**.

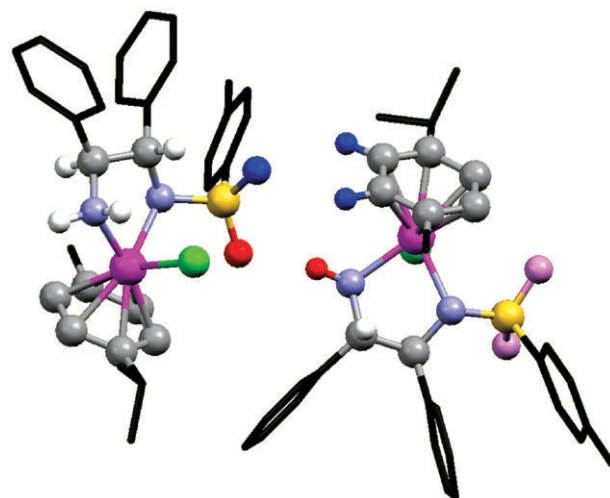


Fig. 2 ONIOM (B3PW91:UFF) geometry for the dimeric structure **1–1**. The atoms treated at the DFT level are represented as balls and sticks, whereas the atoms treated at the MM level are represented as capped sticks and are in black. The short $\text{NH} \cdots \text{O}1$ and $\text{CH} \cdots \text{O}2$ contacts are shown in red and blue, respectively.

(2.59 Å and 2.65 Å) contacts have been highlighted in red and blue, respectively.

The structure of monomeric **1** was also optimized at the ONIOM (B3PW91:UFF) level and the calculated geometry is in excellent agreement with the X-ray data (Fig. 3). The ONIOM geometries were then used in single-point calculations at the B3PW91 level to evaluate the respective energies of dimer **1–1** and monomer **1**. The formation of the dimer was found to be exothermic by $13.4 \text{ kcal mol}^{-1}$, in agreement with the observation of two HBs in the dimeric structure of *ca.* 7 kcal mol^{-1} each. The formation energy of the dimer was also computed, on the ONIOM geometries, within a continuum model for the solvent (CPCM) at the B3PW91 level. The solvents tested were dichloromethane, methanol and acetone and, in each case, the dimer was found to be more stable than the monomer (by 2.6, 1.7 and 1.3 kcal mol^{-1} , respectively).¹¹ There is thus a large electronic driving force towards the

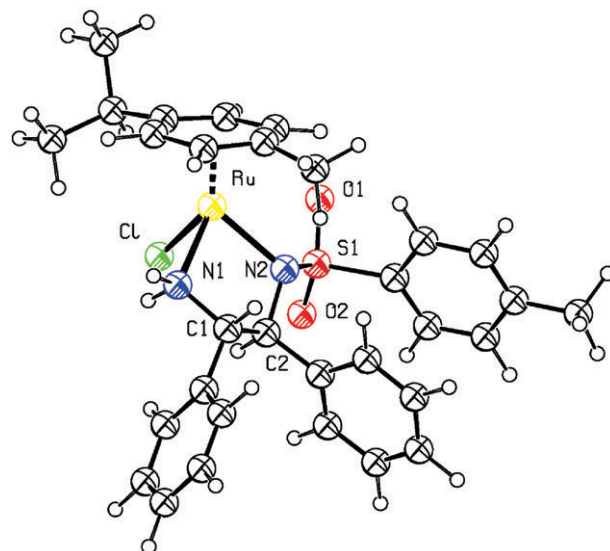


Fig. 3 Optimized structure of **1** at the ONIOM (B3PW91:UFF) level, with numbering scheme. Selected calculated geometrical parameters are [for comparison, values from the experimental structure of **1** (ref. 10) are given in parentheses]: Ru–D 1.687 (1.669); Ru–N1 2.132 (2.116); Ru–N2, 2.140 (2.145); Ru–Cl 2.408 (2.435); N1–Ru–N2 79.6 (79.5); N1–Ru–Cl 79.1 (81.1); N1–C1–C2–N2 54.9 (49.4); Ru–N2–S1–O1 37.0 (27.0) with distances in Å, angles in °, and where D is the centroid of the cymene C6 ring.

aggregation of **1** as a dimer in the gas phase. This tendency to aggregate is still present when the solvent is included and the calculated stabilization energy is not influenced greatly by the value of ϵ_r . The origin of this aggregation likely lies in the very efficient cooperative hydrogen bonding pattern. Aggregates bigger than dimers can form using the interaction between the SO₂ functional group that is not involved in the formation of the dimer and NH and CH moieties belonging to another molecule.

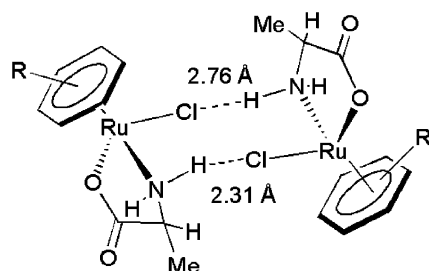
α -Amino acidate compounds **2–5** have $N \geq 1.7$ (entries 12–22 in Table 1). The aggregation tendency of compounds **2–5** is considerably reduced by the substitution of NH₂ by NMe₂ (compare entries 12–14 with 15–17) but is little affected by exchanging cymene for the benzene ligand (compare entries 19 and 21). Aggregates are also present in DMSO-d₆, as indicated in Table 1, entries 18 and 22 for compounds **3** and **5**, respectively. Aggregates of compounds **2–5** may form, owing to intermolecular hydrogen bonds between the chlorine atom coordinated to the ruthenium and the NH for **2**, **4** and **5** (Scheme 2).⁴ The reduced but still considerable aggregation observed for compound **3**, having no NH proton, could be explained by assuming that arene C–H...Cl–Ru interactions are present in solution.

In conclusion, we have reported here unprecedented evidence of the formation of dimers and larger aggregates from the neutral Noyori and α -amino acidate compounds, which are active catalysts for transfer hydrogenation, in the environment where they are used. Further investigations are in progress in order to understand whether or not such aggregation is limited to the chlorine derivatives and whether it plays any role in the catalytic properties.

Experimental

Experimental methods

Compounds **1**,¹⁰ **2–5**¹² and **6**⁷ were synthesized according to the literature. All the ¹H PGSE NMR measurements were performed by using the standard stimulated echo pulse sequence¹² on a Bruker AVANCE DRX 400 spectrometer equipped with a GREAT 1/10 gradient unit and a QNP probe with a Z-gradient coil, at 296 K without spinning. The viscosity values introduced in the modified Stokes–Einstein equation were corrected to take into account both the temperature and the deuteration of the solvents. The D_t of water, necessary to calibrate the gradient intensities, was also interpolated at the corrected temperature. The measurement uncertainty was estimated by performing experiments with different Δ values.¹³ Standard propagation of errors analysis yielded a standard deviation of approximately 2–3% in r_H and 8–9% in V_H and N . Tetrakis(trimethylsilyl)silane (TMSS, $r_{vdW} = 4.28$ Å) was used as internal standard in order to check the accuracy of the measurements. Its van der Waals radius was extremely well reproduced in all solvents with a deviation smaller than 0.18 Å (<4%).



Scheme 2 Intermolecular hydrogen bonding between the amine protons and the chlorine in the pair of diastereoisomers having opposite chiralities at the metal center (ref. 4).

Computational details

All calculations were performed with the Gaussian 98 set of programs¹⁴ with the ONIOM method.¹⁵ The QM part of the calculations was treated within the framework of hybrid DFT (B3PW91)^{16,17} and consisted in the model system (η^6 -C₆H₆)Ru(Cl)(NH₂CH₂CH₂NSO₂H). The ruthenium atom was represented by the relativistic effective core potential (RECP) from the Stuttgart group (16 valence electrons) and its associated (8s7p6d)/[6s5p3d] basis set,¹⁸ augmented by an f polarization function ($\alpha = 1.235$).¹⁹ The chlorine and sulfur atoms were represented by RECP from the Stuttgart group and the associated basis set,²⁰ augmented by a d polarization function.²¹ A 6-31G(d,p) basis set²² was used for all the remaining atoms of the complex (C, H, O, N). The MM part of the calculations consisted in the missing phenyl groups on C1, C2, the *para*-tolyl group on S1, and also of the Me and *i*-Pr substituents on cymene. The UFF force field was used in the MM calculations.²³ Full optimizations of geometry without any constraints were performed on both monomer **1** and dimer **1–1**, followed by analytical computation of the Hessian matrix to confirm the nature of the located extreme as minima on the potential energy surface. The formation energy of dimer **1–1** from monomer **1** was also evaluated at the DFT level on the ONIOM geometries. Single-point energy calculations on the ONIOM optimized monomeric and dimeric structures were performed with the same basis set as described above for the QM part of the ONIOM calculations. The evaluation of the stabilization energy in these single-point calculations was performed at the B3PW91 level, either in the gas phase, or within a continuum description of the solvent as implemented in the CPCM procedure of Barone and Cossi.²⁴

Acknowledgements

We thank the Ministero dell'Istruzione, dell'Università e della Ricerca (MIUR, Rome, Italy), Programma di Rilevante Interesse Nazionale, Cofinanziamento 2002–2003, the COST D24/WG 0014/02 action, the Université Montpellier 2 and the CNRS for support.

References

- (a) R. Noyori and S. Hashiguchi, *Acc. Chem. Res.*, 1997, **30**, 97; (b) M. Yamakawa, H. Ito and R. Noyori, *J. Am. Chem. Soc.*, 2000, **122**, 1446; (c) R. Noyori, M. Yamakawa and S. Hashiguchi, *J. Org. Chem.*, 2001, **66**, 7931.
- (a) T. Ohta, S.-I. Nakahara, Y. Shigemura, K. Hattori and I. Furukawa, *Chem. Lett.*, 1998, **6**, 491; (b) Á. Kathó, D. Carmona, F. Viguri, C. D. Remacha, J. Kovács, F. Joó and L. A. Oro, *J. Organomet. Chem.*, 2000, **593–594**, 299.
- G. Aullón; D. Bellamy, L. Brammer, E. A. Bruton and A. G. Orpen, *Chem. Commun.*, 1998, 653.
- L. C. Carter, D. L. Davies, K. T. Duffy, J. Fawcett and D. R. Russell, *Acta Crystallogr., Sect. C*, 1994, **50**, 1559.
- (a) H. Brunner, M. Weber, M. Zabel and T. Zwack, *Angew. Chem., Int. Ed.*, 2003, **42**, 1859; (b) H. Brunner, M. Weber and M. Zabel, *Coord. Chem. Rev.*, 2003, **242**, 3.
- D. Zuccaccia, S. Sabatini, G. Bellachioma, G. Cardaci, E. Clot and A. Macchioni, *Inorg. Chem.*, 2003, **42**, 5465.
- G. Bellachioma, G. Cardaci, V. Gramlich, A. Macchioni and L. M. Venzani, *J. Chem. Soc., Dalton Trans.*, 1998, 947.
- (a) C. S. Johnson, Jr., *Prog. Nucl. Magn. Reson. Spectrosc.*, 1999, **34**, 203; (b) P. Stilbs, *Prog. Nucl. Magn. Reson. Spectrosc.*, 1987, **19**, 1.
- (a) H.-C. Chen and S.-H. Chen, *J. Phys. Chem.*, 1984, **88**, 5118; (b) P. J. Espinosa and J. G. de la Torre, *J. Phys. Chem.*, 1987, **91**, 3612.
- Van der Waals volume and radius were calculated from the X-ray structure reported in: K.-J. Haack, S. Hashiguchi, A. Fujii, T. Ikariya and R. Noyori, *Angew. Chem., Int. Ed.*, 1997, **36**, 285.
- The reduction of the stabilization energy results from the fact that all the H-bond donors and acceptors are available for electrostatic

interactions with the solvent in the monomeric case while some of them are engaged in "intramolecular" interactions in the dimeric form. Consequently, the solvation energy for the dimer is lower than for the monomer and thus the stabilization energy is decreased.

- 12 (a) D. F. Dersnah and M. C. Baird, *J. Organomet. Chem.*, 1977, **127**, C55; (b) R. Krämer, K. Polborn, H. Wanjek, I. Zahn and W. Beck, *Chem. Ber.*, 1990, **123**, 767; (c) D. Carmona, A. Mendoza, F. J. Lahoz, L. A. Oro, M. P. Lamata and E. San José, *J. Organomet. Chem.*, 1990, **396**, C17.
- 13 (a) M. Valentini, H. Rüegger and P. S. Pregosin, *Helv. Chim. Acta*, 2001, **84**, 2833; (b) B. Binotti, A. Macchioni, C. Zuccaccia and D. Zuccaccia, *Comments Inorg. Chem.*, 2002, **23**, 417.
- 14 M. J. Frisch, G. W. Trucks, H. B. Schlegel, G. E. Scuseria, M. A. Robb, J. R. Cheeseman, V. G. Zakrzewski, J. A. Montgomery, Jr., R. E. Stratmann, J. C. Burant, S. Dapprich, J. M. Millam, A. D. Daniels, K. N. Kudin, M. C. Strain, O. Farkas, J. Tomasi, V. Barone, M. Cossi, R. Cammi, B. Mennucci, C. Pomelli, C. Adamo, S. Clifford, J. Ochterski, G. A. Petersson, P. Y. Ayala, Q. Cui, K. Morokuma, P. Salvador, J. J. Dannenberg, D. K. Malick, A. D. Rabuck, K. Raghavachari, J. B. Foresman, J. Cioslowski, J. V. Ortiz, A. G. Baboul, B. B. Stefanov, G. Liu, A. Liashenko, P. Piskorz, I. Komaromi, R. Gomperts, R. L. Martin, D. J. Fox, T. Keith, M. A. Al-Laham, C. Y. Peng, A. Nanayakkara, M. Challacombe, P. M. W. Gill, B. G. Johnson, W. Chen, M. W. Wong, J. L. Andres, C. Gonzalez, M. Head-Gordon, E. S. Replogle and J. A. Pople, *GAUSSIAN 98 (Revision A.11)*, Gaussian, Inc., Pittsburgh, PA, 2001.
- 15 M. Svensson, S. Humbel, R. D. J. Froese, T. Matsubara, S. Sieber and K. Morokuma, *J. Phys. Chem.*, 1996, **100**, 19357.
- 16 A. D. Becke, *J. Chem. Phys.*, 1993, **98**, 5648.
- 17 J. P. Perdew and Y. Wang, *Phys. Rev. B*, 1992, **45**, 13244.
- 18 D. Andrae, U. Häussermann, M. Dolg, H. Stoll and H. Preuß, *Theor. Chim. Acta*, 1990, **77**, 123.
- 19 A. W. Ehlers, M. Böhme, S. Dapprich, A. Gobbi, A. Höllwarth, V. Jonas, K. F. Köhler, R. Stegmann, A. Veldkamp and G. Frenking, *Chem. Phys. Lett.*, 1993, **208**, 111.
- 20 A. Bergner, M. Dolg, W. Küchle, H. Stoll and H. Preuß, *Mol. Phys.*, 1993, **30**, 1431.
- 21 A. Höllwarth, H. Böhme, S. Dapprich, A. W. Ehlers, A. Gobbi, V. Jonas, K. F. Köhler, R. Stagmann, A. Veldkamp and G. Frenking, *Chem. Phys. Lett.*, 1993, **203**, 237.
- 22 P. C. Hariharan and J. A. Pople, *Theor. Chim. Acta*, 1973, **28**, 213.
- 23 A. K. Rappé, C. J. Casewitt, K. S. Colwell, W. A. Goddard and W. M. Skiff, *J. Am. Chem. Soc.*, 1992, **114**, 10024.
- 24 V. Barone and M. Cossi, *J. Phys. Chem. A*, 1998, **102**, 1995.